Water Research 166 (2019) 115067

Contents lists available at ScienceDirect

Water Research

journal homepage: www.elsevier.com/locate/watres

Synthesized trade-off analysis of flood control solutions under future deep uncertainty: An application to the central business district of Shanghai

Hengzhi Hu [a, 1], Zhan Tian [b, 1], Laixiang Sun [c, d, e, *], Jiahong Wen [a, **], Zhuoran Liang [f], Guangtao Dong [g], Junguo Liu [b]

[a] Department of Environmental and Geographical Sciences, Shanghai Normal University, Shanghai, 200234, China
[b] School of Environmental Science and Engineering, Southern University of Science and Technology, Shenzhen, 518055, China
[c] Department of Geographical Sciences, University of Maryland, College Park, MD, 20742, USA
[d] School of Finance and Management, SOAS University of London, London, WC1H 0XG, UK
[e] International Institute for Applied Systems Analysis (IIASA), A-2361, Laxenburg, Austria
[f] Hangzhou Meteorological Services, Hangzhou, Zhejiang, China
[g] Shanghai Climate Center, Shanghai Meteorological Service, Shanghai, 200030, China

ARTICLE INFO

Article history:
Received 4 May 2019
Received in revised form
5 September 2019
Accepted 6 September 2019
Available online 7 September 2019

Keywords:
Decision-making under deep uncertainty
Urban flood solutions
Cost-effectiveness
Climate change
China

ABSTRACT

Coastal mega-cities will face increasing flood risk under the current protection standard because of future climate change. Previous studies seldom evaluate the comparative effectiveness of alternative options in reducing flood risk under the uncertainty of future extreme rainfall. Long-term planning to manage flood risk is further challenged by uncertainty in socioeconomic factors and contested stakeholder priorities. In this study, we conducted a knowledge co-creation process together with infrastructure experts, policy makers, and other stakeholders to develop an integrated framework for flexible testing of multiple flood-risk mitigation strategies under the condition of deep uncertainties. We implemented this framework to the reoccurrence scenarios in the 2050s of a record-breaking extreme rainfall event in central Shanghai. Three uncertain factors, including precipitation, urban rain island effect and the decrease of urban drainage capacity caused by land subsidence and sea level rise, are selected to build future extreme inundation scenarios in the case study. The risk-reduction performance and cost-effectiveness of all possible solutions are examined across different scenarios. The results show that drainage capacity decrease caused by sea-level rise and land subsidence will contribute the most to the rise of future inundation risk in central Shanghai. The combination of increased green area, improved drainage system, and the deep tunnel with a runoff absorbing capacity of 30% comes out to be the most favorable and robust solution which can reduce the future inundation risk by 85% (±8%). This research indicates that to conduct a successful synthesized trade-off analysis of alternative flood control solutions under future deep uncertainty is bound to be a knowledge co-creation process of scientists, decision makers, field experts, and other stakeholders.

1. Introduction

Climate change presents a significant planning challenge for mega-cities. With a population greater than 10 million, mega-cities are typically the most prominent population and economic centers of their home countries (United Nations, 2018). Observational evidence over the 20th and early 21st century shows that the globally averaged rate of increase in annual maximum daily rainfall intensity was between 5.9% and 7.7% per °C of globally averaged near-surface atmospheric temperature (Westra et al., 2013, 2014). In addition to this global trend, increased urbanization, which is associated with anthropogenic heat and artificial land cover, may lead to an effect of urban rain island in a localized heavy rainfall event. The urban rain island effect means that the center of the city

* Corresponding author. Department of Geographical Sciences, University of Maryland, College Park, MD, 20742, USA.
** Corresponding author.
E-mail addresses: lsun123@umd.edu (L. Sun), jhwen@shnu.edu.cn (J. Wen).
[1] Hengzhi Hu and Zhan Tian contribute equally to this article.

https://doi.org/10.1016/j.watres.2019.115067

receives much more precipitation than the surrounding suburbs. Such an effect has been observed in Tokyo, Japan (Souma et al., 2013; Shimoju et al., 2010; Kusaka et al., 2014), Mumbai, India (Paul et al., 2018), and Shanghai, China (Gu et al., 2015; Liang and Ding, 2017). Looking to the next few decades, it is expected with high confidence that the intensity and/or frequency of extreme daily rainfall will continue to increase, especially in urban areas (IPCC, 2014; Kharin et al., 2007; Westra et al., 2014; Wu et al., 2013).

Mega-cities are therefore positioned to play a leading role in responding to climate change challenges and are in need of knowledge to aid in their planning efforts under deep uncertainty (Aerts et al., 2013, 2014; Rosenzweig et al., 2011). Given the fact that rainfall-derived floods have been one of the most costly and dangerous natural hazards worldwide (Hallegatte et al., 2013; CRED, 2014), it is of great socioeconomic significance to improve our understanding of the changing behavior and impacts of extreme rainfall (Westra et al., 2014) and to find robust solutions for the planning and design of flood protection infrastructures (Löwe et al., 2017). There is a large body of literature assessing the inundation risk under future extreme precipitation scenarios (e.g., among others, Huong and Pathirana, 2013; Jenkins et al., 2017; Muis et al., 2015; Poelmans et al., 2011; Sekovski et al., 2015; Teng et al., 2017; Wu et al., 2018). However, as pointed out by Löwe et al. (2017), such scenario-based evaluations are difficult to apply for planning and design purposes owing to their heavy simulation loads and are therefore typically performed only for a few selected scenarios. Few studies have provided a planning-supporting tool which takes into account the entire cascade of factors from the uncertainties of future urban rainfall behavior, to the physical and economic damages resulting from extreme rainfall events, and to the cost-effectiveness of alternative mitigation options, allowing for a synthesized trade-off analysis of flood control solutions and pathways. This study aims to address this challenge by developing such a synthesized trade-off analysis tool for supporting flood-control planning in Shanghai and other growing megacities such as Shenzhen, Guangzhou, Ho Chi Minh City, São Paulo, Mumbai (Bombay), Dhaka, and Jakarta.

Our approach follows the tradition of the bottom-up decision supporting frameworks, which have a strong comparative advantage in handling deep uncertainties. Of many bottom-up or robustness-based decision supporting frameworks, the following four have achieved increasing popularity: Dynamic Adaptive Policy Pathway (DAPP) (Haasnoot et al., 2012), Information-Gap (Info-Gap) (Ben-Haim, 2004), Robust Decision Making (Lempert and McKay, 2011; Lempert et al., 2013) and Many-Objective Robust Decision Making (MORDM) (Kasprzyk et al., 2013). The construction of these frameworks can be generalized into the following four sequential steps: identifying decision alternatives, sampling the state of affairs, specifying robustness measurements, and performing scenarios discovery to identify the most important uncertainties (Hadka et al., 2015). A successful implementation of these four steps is bound to be a knowledge co-creation process, which emphasizes the generation of useable science for decision-making through sustained and meaningful dialogue between scientists, policy makers, and other stakeholders (Clark et al., 2016; Meadow et al., 2015; Liu et al., 2019). Co-creation is composed of interlinked processes of co-design and co-production (Mauser et al., 2013; Voorberg et al., 2015). The former encompasses scoping of broader research problems and specific project objectives and goals. It ensures that scientists properly understand stakeholder needs and leads to higher stakeholder trust in project results. Knowledge co-production entails the generation of new knowledge through processes that integrate stakeholder and disciplinary (i.e., climate science, hydrology, economics, decision science) scientific expertise. It facilitates the incorporation of stakeholder latent knowledge into the overall scientific synthesis and builds stakeholder capacity to use the project outcomes in decision-making (USGCRP, 2014; Clark et al., 2016).

In this research, we had kept sustained and meaningful dialogues with sectoral experts and decision makers in each key stage of the research for the following shared purposes: (a) scoping the research problems and setting project objectives and goals; (b) knowing about the current protection standards, better understanding the potential vulnerabilities, and selecting the right solutions; (c) finding meaningful approximate methods to grasp such complex issue as the drainage capacity decrease caused by sea-level rise and land subsidence, and identifying priorities and approximation margins in data-model fusion process. With the help of these dialogues, we added to the upstream and midstream of the above “supply chain” the entire cascade of factors that drive flood hazards and interact with the mitigation and control measures. We opted to use the simple and speedy SCS Runoff Curve Number method (Chung et al., 2010; Mishra and Singh, 2003; Chen et al., 2016) as the core of our inundation model to bridge the gap between detailed risk assessment simulations existing in the literature and the requirements of planning applications for science-informed cost-effectiveness comparison across all plausible solutions. We implemented this framework to the reoccurrence scenarios in the 2050s of a record-breaking extreme rainfall event in central Shanghai. To build future extreme inundation scenarios, we focused on three uncertain factors, which are precipitation, urban rain island effect and the decrease of urban drainage capacity caused by land subsidence. To carry out a synthesized trade-off analysis of potential solutions under future uncertainty, we examined the risk-reduction performance and cost-effectiveness of all possible levers across different scenarios.

2. Materials and method

2.1. The case-study city and event

Shanghai, with a territory of 6,340 km^2, provides residence to 24.1 million population in 2018. Shanghai has been the arguably most prominent economic and financial center of China since the early 1900s and is now aiming to be one of the most important economic, financial, shipping, and trading center of the world. However, as shown in Fig. 1, Shanghai is surrounded by water on three sides, to the east by East China Sea, to the north by Yangtze River Estuary, and to the south by Hangzhou Bay. In addition, Huangpu River, a tributary of Yangtze River, runs through the center of Shanghai. The geological profile of Shanghai is mostly composed of soft deltaic deposit. The annual rainfall is about 1200 mm/yr, with 60% falling during the flooding season from May to September (He and Zhao, 2009; He, 2012; Yuan et al., 2017). The analyses of He and Zhao (2009), He (2012), and Yuan et al. (2017) based on daily observational records over 1981–2010 indicated that torrential rainfall (cumulative precipitation > 30 mm/day) in Shanghai are often intensely concentrated within a period of 12 h or less, with an occurrence frequency of 18–23 per year in terms of five-year moving average. The five-year moving average value of extraordinary torrential rainfall (cumulative precipitation > 100mm/12 h) ranges one to four annually. As a consequence, the most devastating hazard in Shanghai has been torrential rainfall-induced inundation, which has led to transportation and other social disruptions annually, caused significant economic losses and endangered urban safety. It is worth highlighting that the solution district as marked in Fig. 1, which is the central business district (CBD) of Shanghai, has the almost lowest elevation in comparison with other districts in the study area and in also Shanghai. Therefore, the performance evaluations of flood control solutions in this study will

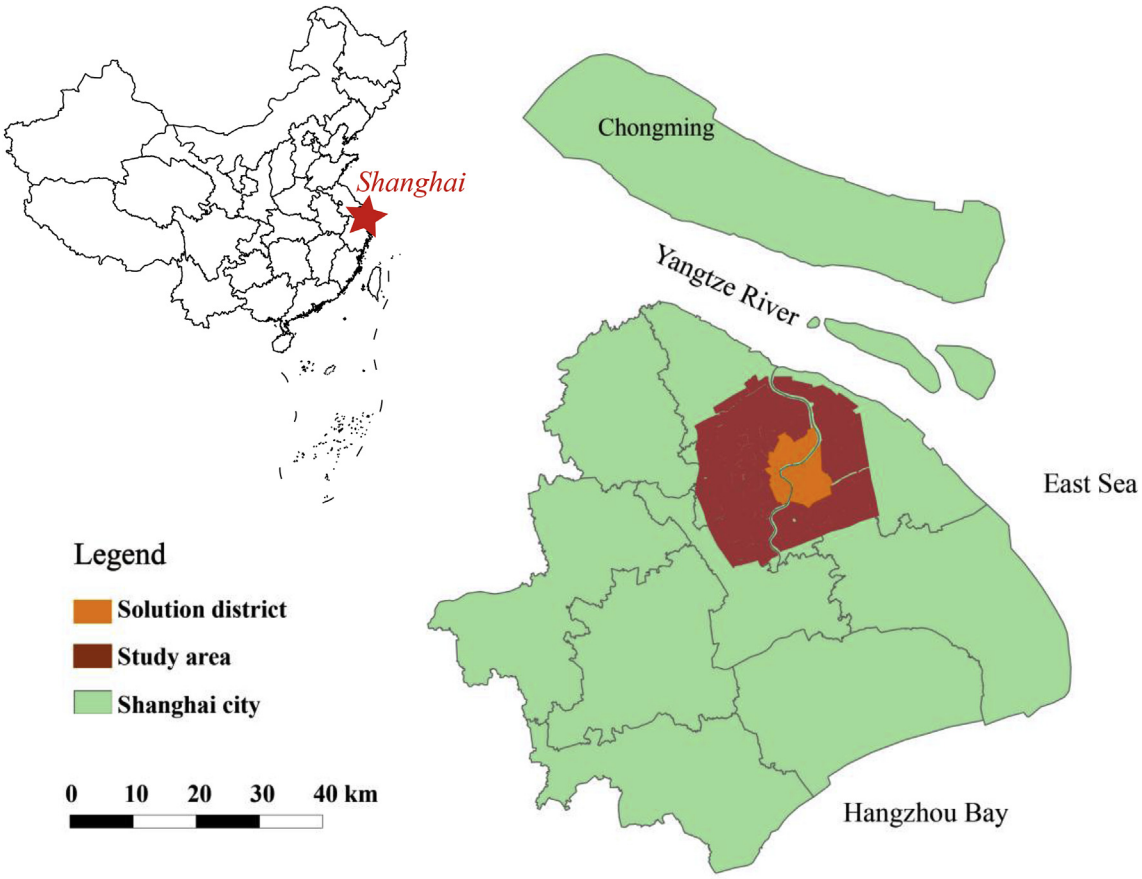

Fig. 1. Shanghai and the study area.

focus on this CBD area.

Looking forward to the coming decades, global warming as a mix of rising temperatures and unstable climate tends to increase the probability of heavy rainfall risks in coastal cities like Shanghai (Chen et al., 2017; Jiang et al., 2015; Lee et al., 2014; Li et al., 2016; Wu et al., 2018). This increasing probability, combined with the trends of sea-level rise and land subsidence which reduce the capacity of existing urban drainage systems, leads to a great concern on the increase of the inundation risk in coastal cities by policy makers, scientists, and the public. While it is recognized that the current flooding control infrastructure in Shanghai would not be sufficient in defending the city against future inundation risk, there is an urgent need for developing a synthesized trade-off evaluation tool to support flood-control planning in Shanghai.

This study paid a special attention to a record-breaking event of convectional rainstorm, which took place during 17–19 h on the 13th of September 2013 and had an intensity record of 130.7 mm in an hour in the study area of Shanghai (Fig. 1), being 20 mm higher than the historic record in Shanghai. The event also had a sharp mark of urban rain-island effect – the extreme rainfall concentrated in the study area (Fig. 1). This event caused severe inundation in the main roads in Pudong CBD region and the temporary out-of-service of the Century Avenue metro station, which is a hub of four metro lines. As a consequence, hundreds of thousands of people were stuck during the evening rush-hour period. This extreme event exposed the vulnerability of the central Shanghai in inundation risk management. Therefore, it can serve as an informative baseline case for testing the impact of future reoccurrence of this event on central Shanghai under a changing climate.

2.2. Methods

Fig. 2 depicts our model-coupling process across the entire cascade of factors that drive flood hazards and interact with the mitigation and control measures. The first major step of the process is to quantify three uncertain factors, which features the future reoccurrence of the 13 September 2013 rainstorm event including spatial rain pattern and rain island effect, and the decrease of urban drainage capacity. The second major step is to simulate the inundation depths and areas for both the baseline event (validation of the Urban Inundation Model) and each of scenario using the Urban Inundation Model. The third major step is to specify various mitigation measures and to evaluate the risk-mitigation performance of these measures under each inundation conditions from step 2. The fourth major step includes the calculations of economic costs of various mitigation measures and then the comparative analysis of cost-effectiveness of all specified mitigation measures. The rest of this section will explain each of the above steps in more details.

2.2.1. Quantification of the three uncertain factors

Observational data at 11 representative meteorological stations in Shanghai showed that the number of extraordinary torrential rainfall events per year (in terms of five-year moving average) did not present an obvious trend during 1960–2010. However, these data did show that the extreme precipitation values (daily rainfall > 99th percentile) exhibited an increased trend at all of the 11 stations, with the slope ranging between 1.31 and 4.16 mm/day (also see, Wang et al., 2015). We had run PRECIS 2.0 regional climate model of UK Met Office Hadley Center for the East China region

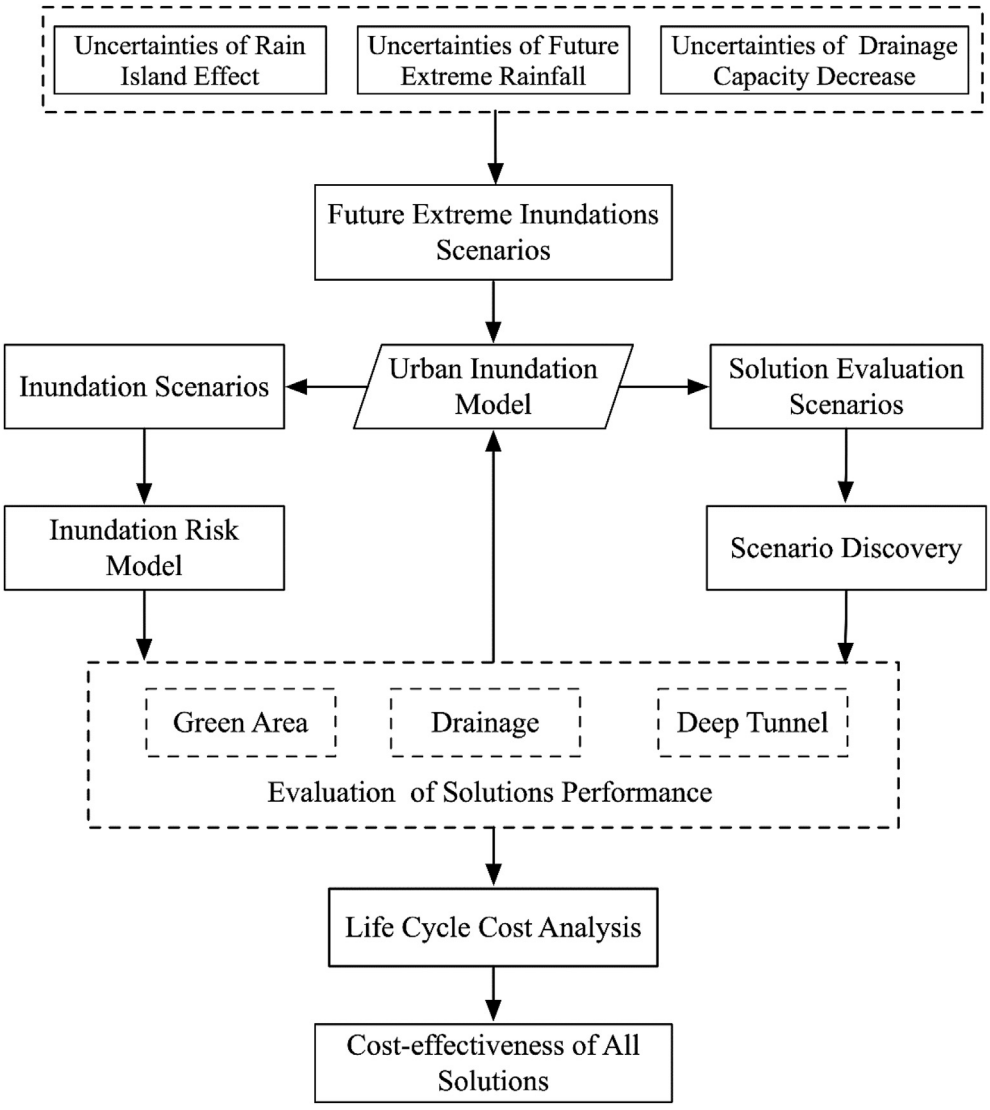

Fig. 2. Coupling flood model, risk model and evaluation model in many plausible scenarios: flow chart.

with the spatial resolution of 25 km under both the baseline climate over 1981–2010 and the RCP4.5 scenario over 2041–2060 (denoted as the 2050s). PRECIS stands for "Providing REgional Climates for Impacts Studies" and is designed for researchers (with a focus on developing countries) to construct high-resolution climate change scenarios for their region of interest (Hadley Centre, 2018). Representative Concentration Pathway (RCP) 4.5 is a scenario that stabilizes radiative forcing at 4.5 W m^{-2} (approximately 650 ppm CO_2-equivalent) in the year 2100 without ever exceeding that value (Thomson et al., 2011). The results indicate an increase of the extreme precipitation value (daily rainfall > 99th percentile) by above 10% from the baseline climate to the 2050s. Considering the observed historical trend in Wang et al. (2015) and the uncertainties of the future climate, we assume that the increase rate (α) of the future precipitation in an extraordinary torrential rainfall event in Shanghai by the 2050s will range between 7% and 18%, in comparison with a similar event under the baseline climate. In Section S1 of the Supplementary Material, we provide more details on the estimation of this range based on multiple climate model projections and RCP scenarios. In our case study of the reoccurrence of the extreme rainfall event on 13 September 2013, this means that an amount of 7%–18% additional precipitation will be added to the gauge's value of the baseline event for generating more inclusive and plausible scenarios.

In terms of spatial distribution, Liang and Ding (2017) employed the hourly precipitation records of the same 11 representative meteorological stations as employed in our research in Shanghai over 1916–2014 to investigate the spatial and temporal variations of extreme heavy precipitation and its link to urbanization effects. Their analysis showed that the long-term trends of the frequency and total precipitation of hourly heavy rainfall across the 11 stations exhibited obvious features of urban rain-island effect, with heavy rainfall events increasingly focused in urban and suburban areas. In more details, the total precipitation amounts of heavy rainfall event over central urban (Pudong and Xujiahui) and nearby suburban (Minhang and Jiading) sites increased by the rates of 21.7–25mm/10yr. In sharp contrast, the trends at rural stations are not clear and, in some cases, even show a slight reduction. Based on these findings and the clear urban rain-island feature of the 13 September 2013 rainstorm event, we conducted face-to-face discussions with climate experts at Shanghai Meteorological Services with regard to the future dynamics of such urban island effect. The

discussions came with an agreement that the urban rain island effect will have a margin of increase (β_1) by 10%–20% in the case of future reoccurrence over central urban sites (Xujiahui and Pudong) by the 2050s, but will have a small margin of decrease (β_2) by −0.076% to −0.038% at other stations.

With the help of above assumptions, we can establish a large set of scenarios for the future reoccurrence of the extreme rainfall event on 13 September 2013. For example, by taking any value within the above-assumed intervals of the increase rate of rainfall extremes (α) and urban rain island effect (β_1 and β_2) respectively, we can apply these values to the observed baseline precipitation amount at each of the 11 representative rain gauges to generate one scenario at the gauge level. Then, we can interpolate this gauge-level scenario into spatial rainfall pattern across the whole Shanghai city area.

Shanghai has been experiencing land subsidence for years, mostly owing to groundwater extraction and increasing number of high-rise buildings. Anthropogenic urban land subsidence in combination with the global warming induced sea level rise will exacerbate the impact of extreme rainfall and reduce the capacity of drainage system. It is estimated that a relative rise of sea level by 50 cm (the height of land subsidence plus elevation of sea level rise), which is highly likely by the 2050s in Shanghai, would reduce the capacity of current river embankment and drainage systems by 20–30% (Liu, 2004; Wang et al., 2018). To take into account the uncertainties in sea-level rise, land subsidence, and other degradation factors of the drainage systems, we assume that the decreasing rate of existing drainage system capability (γ) would range between 0% and 50%.

Dividing the intervals of α, β_1, β_2, and γ into 100 equal intervals would generated 10^8 combinations of plausible values of the uncertain factors, too many for a meaningful analysis. To select a manageable and representative sample from these 10^8 combinations, we implemented the Latin Hyper Cube (LHC) sampling method in the R programming environment. The LHC is a randomized experimental design that explores the whole input space for the fewest number of representative points in sample (Lempert et al., 2013). In this way, we generate 100 random scenarios of the future reoccurrence of the extreme rainfall event on 13 September 2013.

2.2.2. The Urban Inundation Model and its validation

We developed the Urban Inundation Model (UIM) using Shanghai's data to assess urban flooding risk under various extreme precipitation scenarios. There is a large number of rainfall–runoff methods in the literature. Most of them require intensive input data, demanding calibration, and expansive computing efforts (Chung et al., 2010; Mishra and Singh, 2003). In contrast, the Soil Conservation Service Curve Number (SCS–CN), which is also termed as the Natural Resource Conservation Service Curve Number (NRCS-CN) method, is globally popular for its simplicity, stability, predictability, and ease of application for gauged and ungauged watersheds (Chung et al., 2010; Mishra and Singh, 2003; Chen et al., 2016). Given the fact that our comprehensive evaluations of thousand combinations of inundation scenario and mitigation measures require for running the rainfall–runoff module thousands of times, the SCS-CN method becomes the preferred choice for being the core of the UIM. The UIM uses the SCS-CN urban runoff method to estimate the rainfall loss and surface runoff, matched with the local elevation data and spatial urban drainage capacity. The SCS-CN method is based on an empirical proportionality relationship, which indicates that the ratio of cumulative surface runoff and infiltration to their corresponding potentials are equal. Hooshyar and Wang (2016) provided the physical basis of the SCS-CN method and its proportionality hypothesis from the infiltration excess runoff generation perspective. Chung et al. (2010) amended the SCS method to allow for the theoretical exploration of the range in which the CN usually falls. In Section S2 of the Supplementary Material, we provided technical details of the SCS-CN method adopted in the UIM and the localization of key parameters.

The input data required by the UIM includes: (1) Gridded precipitation data, which were generated by spatial interpolation of site observations (baseline) and the site-level reoccurrence scenarios of the extreme rainfall event on 13 September 2013 to 30m resolution grids. (2) Soil and land use data, which are mainly used for determining the CN values of land use type, soil infiltration characteristics (soil type) and pre-soil moist condition (AMC). Soil data was obtained from the Harmonized World Soil Database (HWSD) (Fischer et al., 2008), with a spatial resolution of 1 km. Land use data was from the 2014 satellite data inversion provided by the Institute of Geographic Sciences & Natural Resources Research of the Chinese Academy of Sciences, with a spatial resolution of 30 m. (3) Digital Elevation Model (DEM) elevation data, which was obtained from the ASTER satellite 30m resolution data, using the filling process to remove some false depressions according to the land use data. Considering that the residential and commercial land generally have a certain step height, we made a correction on the residential and commercial land terrain by adding 150 mm. (4) The map of the municipal underground pipe network is unavailable. However, considering that the underground pipelines are typically located along the street networks, Shanghai Water Authority provided drainage unit map and the approximation of the pipe capacity enclosed by streets boundaries.

To validate the spatial performance of the UIM's baseline simulation, we employed the public-reported waterlogging point data, provided by the Shanghai Police Office, on 13 September 2013. This database showed 760 reported flood points during 17–19 h on the 13th of September 2013 and most of them were in the solution district of our Study area. Fig. 3 compares the spatial patterns of simulated inundation by the UIM and the public-reported waterlogging points. It shows a very good match in terms of area coverage in the solution district.

To further check the accuracy of the UIM simulation in terms of water depth, we ran InfoWorks (v 8.5, developed by Innovyze, 2018; Han, 2014; Han et al., 2014) simulation of the same event for the same solution district using the same input data in the UIM hydrological module. InfoWorks ICM is an integrated catchment modeling software and has been widely used in urban flooding simulations in the business world. The InfoWorks ICM enables to create an integrated model for 1D hydrodynamic simulations and 2D simulations both above and below ground drainage networks in urban area. The 1D and 2D integration model gives a holistic view of complete catchment as it happens in reality, and many works were generated in a small spatial zone as a number of blocks or a community. However, its triangle based 2D mesh zone sacrifices the calculation speed at a city district level. In our test, the ground model (DEM) was meshed in 2D Zone with triangle unit area between 1000 m^2 to 5000 m^2, and the different drainage unit is modelled in different infiltration surface considering their drainage capacity. The comparison statistics shows that both the UIM and InfoWorks ICM simulations have the similar maximum depths (840 mm versus 800 mm) and similar size of inundated area (20 km^2 versus 21 km^2).

2.2.3. Characteristics of solutions

Although Shanghai has already built up a comprehensive flood and inundation protection system, additional solutions are still needed to address the inundation issue in the future. Aiming to increase the current protection standards, a series of hydraulic

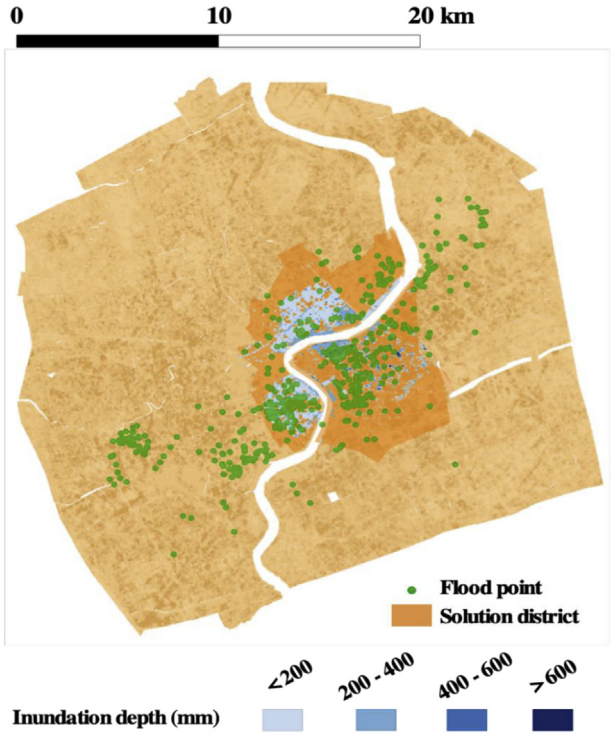

Fig. 3. Validation of Shanghai UIM simulation using public-reported waterlogging points.

engineering projects have been planned or are under construction, which includes the upgrading of old drainage pipelines, construction of deep tunnels under the riverbed of the lower reach of Suzhou Creek, and other green infrastructure projects. In line with the 13th five-year plan of Shanghai on flooding control (Shanghai Municipal Government, 2017) and the ongoing hydrological engineering projects, we evaluate three sets of solutions, the increase in the capacity of drainage systems by the planned rates, the increase of green area by various rates, and the construction of deep tunnels with varying capacities. To make these solutions geographically compatible, we assume all the solutions are implemented in the same core region within the study area (i.e., the solution district), which is about 70 km^2 and mainly consist of the core CBD region in Shanghai.

Drainage. The study area is divided into 284 drainage units by Shanghai Water Authority. These units are categorized by three types of standards in terms of drainage capacity: 27 mm/h, 36 mm/h and 50 mm/h, based on the current designed capacity of local return period of 1, 2, and 5 years. According to the 13th five-year plan for water management and flood control in Shanghai (Shanghai Municipal Government, 2017), the current drainage standard will be raised in central Shanghai. Following this plan and consultations with water and urban planning authorities, we assume that the drainage capacity in the whole solution district will be upgraded to the highest standard: 50 mm/h. This means that the extent of standard rising is location specific.

Green Area. The Shanghai Municipal Government has shown a strong willingness to improve the urban ecological environment through augmented funding for preserving and expanding public green areas. Statistical data show that both urban green area coverage and forest coverage have been increasing annually in last 25 years (Statistical Yearbook of Shanghai, 2010, 2013, 2014, 2015, 2016). It is anticipated that future investment in green area will continue to rise. In addition to their great contribution to air cleaning and urban environmental improvement, green areas also play an important role in rain-water harvesting and reducing urban surface runoff. The Municipal Government has strongly promote "sponge city" guideline of increasing the green and permeable area by building green roofs and porous pavement, and by tree and grass planting in public spaces. In line with this guideline and Shanghai Master Plan 2017–2035 (Shanghai Urban Planning and Land Resource Administration Bureau, 2018), we assume that about 40% of the existing impermeable and moderately permeable (with 50% permeability) area in the Solution District, equivalent to about 30 km^2, will become permeable (with 70% permeability) by the 2050s. We down-scale the district-specific requirements of the "sponge city" guideline and Master Plan onto the drainage unit level. This means that the distribution of the green area is specific to each drainage unit, but there is no locational alternatives. The conversion from the impermeable area and moderately permeable to permeable is modelled in the UIM through changes in the CN. In more detail, the permeability conversion is implemented by lowering the values of CN in the SCS model from 98 (impermeable) and 86 (moderately impermeable) to 80 in the corresponding areas.

Deep Tunnel. The construction of deep tunnels will increase the urban capacity to minimize the surface runoff and thus reduce the inundation impact. Shanghai initiated the Suzhou Creek deep tunnel project in 2016 with a designed length of 15.3 km, which aims to serve an area of 58 km^2 mostly in the study area. The target of the deep tunnel is to raise the drainage standard from 1 year to 5 years return period in its serving area and to well manage the rainstorm with a 100 year return period, bringing no regional transportation abruption and keeping the water depth on roads no more than 15 cm. The first stage of the project is planned to be completed by the end of 2020, followed by the construction of supporting systems (2nd stage), and then long-term extension stage. Given the fact that construction of a complete system of deep tunnel water storage, sedimentation and purification, and discharge by pumping is financially expansive and time consuming, we designed to test three levels of the capacity of the deep tunnel project: handling 30%, 50% and 70% (Tun30, Tun50, and Tun70) of remaining floodwater after those handled by the existing infrastructure in the baseline run of the UIM (the rainfall event on 13 September 2013). These three levels of capacity are equivalent to satisfactorily serving an area of 21 km^2, 35 km^2, and 49 km^2 with the standard of 5-year return period in the solution district, respectively.

2.2.4. Performance evaluation

For each solution or a combination of solutions, we evaluate its beneficial performance by the metric of the risk reduction rate (RRR). The hydrological effectiveness (as measured by the RRR) per unit of abatement cost is employed to evaluate the cost-effectiveness of different solutions.

Flood-induced casualties and physical damage to buildings, indoor/outdoor belongings, infrastructure and natural resources constitute the direct loss, which, in general, can be measured definitely by monetizing across all assets. Damage incurred by a physical asset was calculated as a percentage of its value, and the function relating flood depths to this proportion is called a depth-damage curve, which considers the relationships of flood characteristics (such as water depth, flow velocity, flood duration, etc.) and damage extent (either by the absolute damage values or the relative damage rates) in the elements at risk.

The study area is located in the CBD with a high density of residential and commercial properties. We opted to focus on direct damage loss resulting from inundation. Loss caused by the possibility of structural damage from the velocity of incoming water is not estimated. In other words, we specifically look at the categories

of damage to buildings (residential, commercial), loss of belongings (indoor) and economic disruption so as to examine the direct losses caused by urban inundation. We evaluated the inundation risk based on the following equation (ISO Guide 31000, 2009).

$$Risk = Hazard \times Exposure \times Vulnerability. \quad (1)$$

Section S3 in Supplementary Material presents the procedures to quantify each element in Eq. (1). The risk reduction rate (RRR) by a specific set of mitigation solutions is calculated as the percentage difference between the risk under the given extreme-rainfall scenario without adding any solution (R_N, "not treated") and the risk under the same extreme-rainfall scenario with the specific set of solutions (R_T, "treated") as specified in Eq. (2).

$$RRR = \frac{R_N - R_T}{R_N} \times 100\%. \quad (2)$$

Benefit-cost ratio is often used in public investment analysis. However, it is not easy to accurately quantify the public benefits of inundation abatement. In contrast, the cost-effectiveness, which measures the hydrological effectiveness per unit of abatement cost, can be quantified with confidence and can serve the purpose of comparison across different scenario-solution combinations (Chui et al., 2016; Liao et al., 2013). We use the RRR from Eq. (2) to measure the hydrological effectiveness. For cost estimation, a life cycle cost analysis is necessary because the solutions differ in initial cost, annual operation and maintenance cost, salvage value and particularly, lifespan. We calculate the present value (in 2013 RMB) of the life cycle cost of a solution (or a combination of solutions). In the calculation, we assume that the discount rate in Shanghai is 5% as justified in Ke (2014). Section S4 in Supplementary Material presents more information on cost estimations of the basic solutions.

3. Result

3.1. Inundation simulation

The 100 sampled scenarios of the future reoccurrence of the 13 September 2013 rainstorm event, as selected in Section 2.2.1, were simulated based on the current flood control infrastructure in the whole study area (reference runs). Two indexes were presented herewith to show the uncertain extent of the inundation: (1) average inundation depth in the solution district, and (2) the average 90th percentile depth, which features the average depth of the upper decile of the most inundated drainage units within the solution district.

Fig. 4 shows the variation across the 100 scenarios. It appears that the second index increases in direct correspondence to the first one. The maximum and minimum of both indicates arrive in Sc-11 and Sc-53, with the maximum and minimum of the first index being 97.68 mm and 17.65 mm, and those of the second being 543.2 mm and 176.5 mm, respectively. The variation of the average inundation across the 100 scenarios are large and its minimum is only 18% of its maximum, whereas the minimum of average 90th percentile inundation equals 67.5% of its maximum.

All scenarios add increments to both the baseline inundation depth and area. Sc-11, Sc-3 and Sc-53 show the worst, moderate and mild increments (Fig. 5). The hotspot inundation areas are mostly in the CBD region where agglomerations of numerous properties and business are located along the banks of the Huangpu River. The affected area in Sc-11 is significant large than that in both Sc-3 and Sc-53. In terms of inundation depth, many grids in Pudong District show high values in all three scenarios. In the worst case Sc-11, the inundation depth reaches as high as 1420 mm in some grids in Pudong, which is 750 mm higher than the maximum depth in the baseline simulation, and the inundated area is more than doubled in comparison with the baseline. Even in mild increment scenario like Sc-11, there are still some grids in the CBD region where the average 90th percentile water depth can be more than 1000 mm, implying a high potential risk in the 2050s (Fig. 5).

3.2. The performance of solutions in reducing inundation

To evaluate the performance of solutions in reducing inundation, we re-run the simulations of the 100 sampled scenarios based on the following five flood control solutions and their various combinations in the solution district: drainage capacity enhancement (drainage), green area increase (green), deep tunnel with 30% runoff absorbed (Tun30), deep tunnel with 50% runoff absorbed (Tun50), deep tunnel with 70% runoff absorbed (Tun70). A performance evaluation based on average depth and average 90th percentile depth shows that: 1) most of the solutions perform well in the mild increment cases (e.g. Sc-53), in which the solutions can wipe out the inundation water generally; (2) in the worst rainfall increment cases (e.g. Sc-11), the performance of solutions varied from good to very poor; 3) the depth reduction range of all solutions across the 100 rainfall scenarios is from 8% (e.g., "drainage" in Sc-11) to 98.9% (e.g. Tun50, "Drainage"+"Green"+Tun30, and Tun70 in Sc-53).

Because of the heavy precipitation (more than 140 mm) in a short duration (less than 3 h), and in addition, the decrease of the drainage capacity (γ) caused mainly by sea-level rise and land subsidence, the drainage improvement solution alone is unable to meaningfully reduce the water level in most cases, especially in the worst cases. A key aspect of the "sponge city" is to increase green area which can in turn increase the rainwater infiltration and residence time. However, increased green space alone does not perform well in the worst increment scenario as well. The implementation of a deep tunnel solution shows an advantage in reducing the surface runoff, especially during a rainfall peak by absorbing 30%, 50% and 70% of remaining runoff after the absorption in the baseline UIM run. By combining different solutions together, we find that the combination of green area and drainage is able to improve the performance in the worst-case scenario and the performance increases significantly once adding the deep tunnel solutions in.

The risk reduction rate (RRR) by a specific set of solutions from the risk level under an extreme-rainfall scenario without adding any solution is calculated using Eq. (2) to determine the performance of this set of solutions. Fig. 6 shows the RRRs of seven selected solutions − green area increase (GA), drainage enhancement (Dr), Tun30, Dr + GA (D + G), Tun50, Dr + GA + Tun30 (D + G + Tun30), and Tun70 − under each of the 100 rainfall scenarios, with reference to different level of γ, the parameter featuring the uncertainties in the decreasing rate of existing drainage system capability caused by sea-level rise, land subsidence, and other degradation factors. Fig. 6 also shows the average inundation depth across the combinations of solution and rainfall scenarios at the given level of γ. In Fig. 6 we can see that the average inundation depth increases almost linearly with the reduced drainage capacity (γ) and furthermore there is a strong negative correlation between the average inundation depth and the risk reduction rates of any given set of solutions when moving with γ. In fact, similar strong negative correlation also exists between the average inundation depth and risk reduction rate of any a given combination of solution and rainfall scenario when moving along the γ axis. By contrast, the correlation between future precipitation and the inundation depth is much weak. This set of results indicates that drainage capacity decrease caused by sea-level rise and land

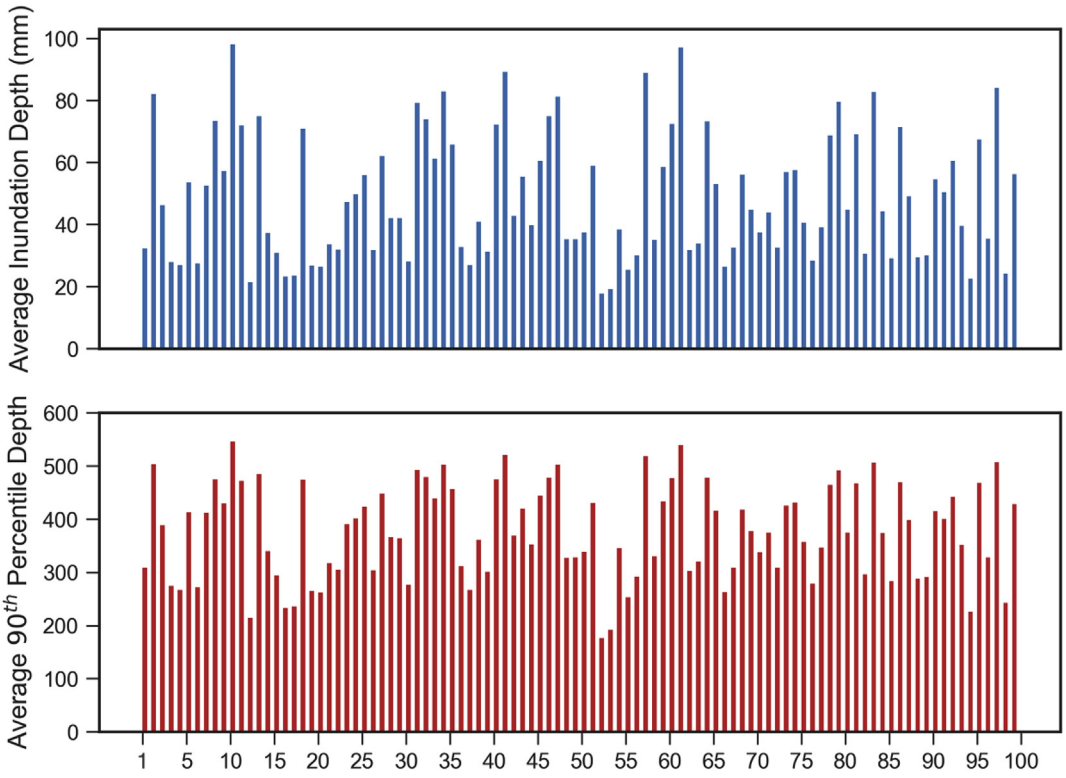

Fig. 4. Average inundation depth (upper figure) and average 90th percentile depth (lower figure) in the 100 inundation scenarios (scenario ID number on the x-axis).

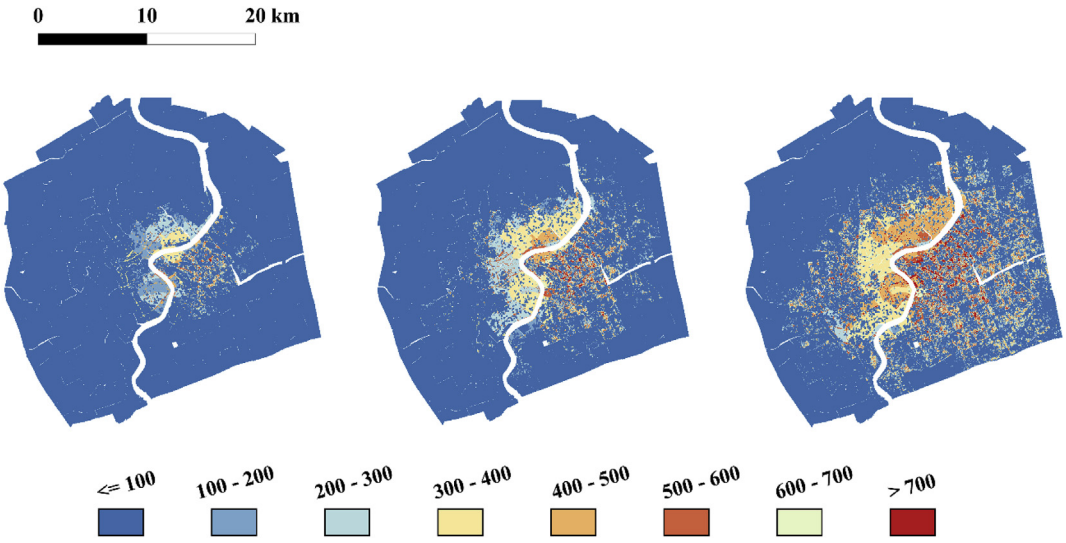

Fig. 5. Comparison of Inundation area and depth (mm): Sc-53 (left), Sc-3 (middle), Sc-11 (right). The α, β_1 and γ values of these three scenarios are presented in Table S2 of SM. The corresponding damage/loss maps are presented in Fig. S1 of SM. (For interpretation of the references to colour in this figure legend, the reader is referred to the Web version of this article.)

subsidence will play a dominant role in worsening future inundation risks in Shanghai.

Fig. 7 displays the box plots of the RRR results over seven selected sets of solutions. It shows that the RRR performances of the first two solutions, i.e. "drainage capacity enhancement" and "green area increase", are the lowest in comparison with other solutions and are statistically similar. The third and fourth solutions, i.e., "deep tunnel with 30% runoff absorbed" and "drainage enhancement + green area expansion," are able to reduce the inundation risk by a large margin on average, but their performances are very dispersed with poor performances in the worst case scenarios. The remaining three solutions, i.e., "deep tunnel with 50% runoff absorbed", "drainage enhancement + green area expansion + deep tunnel with 30% runoff absorbed", and "deep tunnel with 70% runoff absorbed", are much better performers and the performances of the last two solutions are statistically reliable even in the worst case scenarios.

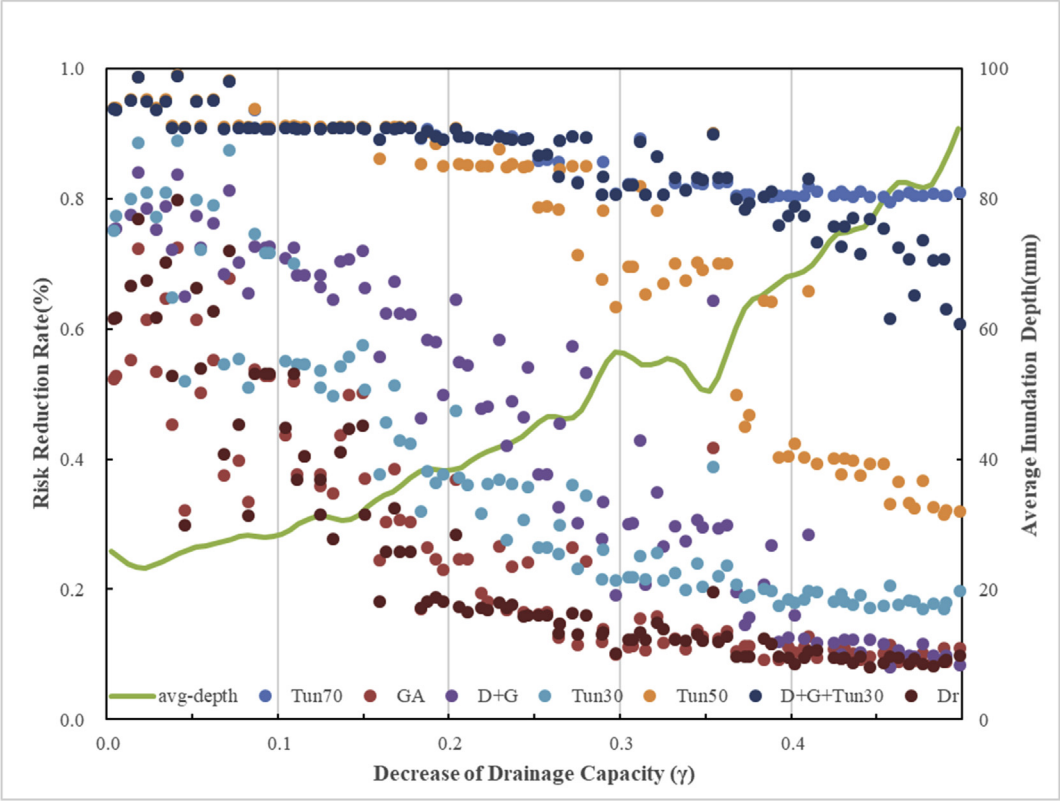

Fig. 6. Risk reduction rate of the seven selected strategies and the average inundation depth across the combinations of solution and rainfall scenarios at the given level of γ. Tun70: deep tunnel with 70% runoff absorbed under the baseline; GA: green area expansion; D + G: drainage enhancement + GA; Tun30: deep tunnel with 30% runoff absorbed under the baseline; D + G + Tun30: drainage enhancement + green area + Tun30; Tun50: deep tunnel with 50% runoff absorbed under the baseline; Dr: drainage enhancement. (For interpretation of the references to colour in this figure legend, the reader is referred to the Web version of this article.)

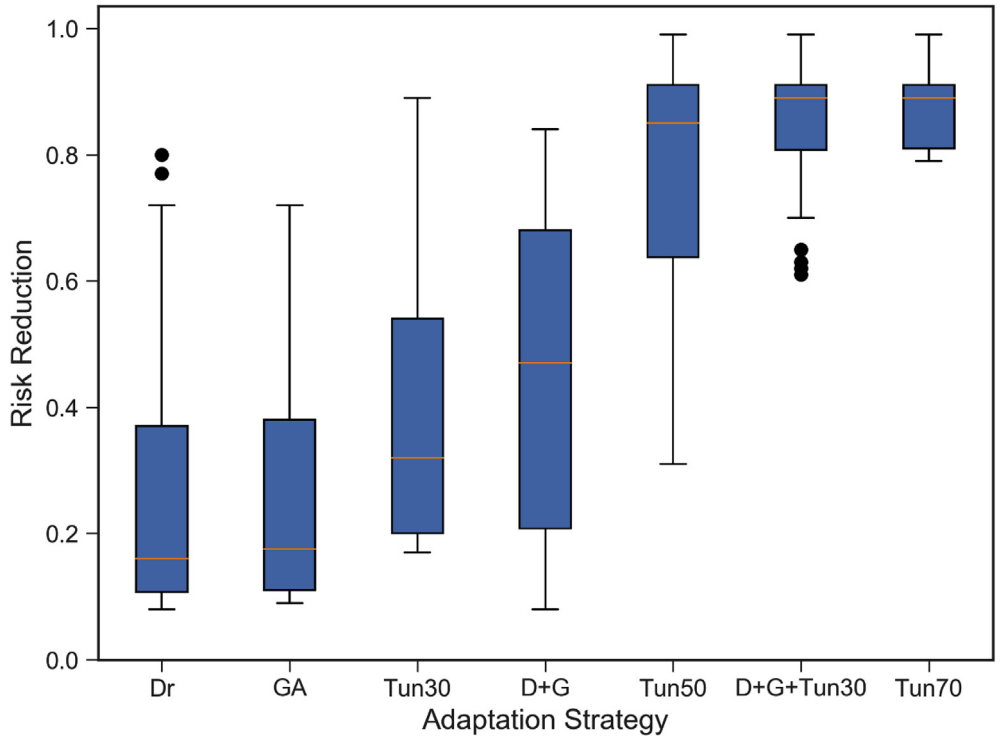

Fig. 7. Box plots of potential risk reduction rates. Dr: drainage capacity enhancement; GA: green area increase; Tun30: deep tunnel with 30% runoff absorbed; D + G: Dr + GA; Tun50: deep tunnel with 50% runoff absorbed; D + G + Tun30: Dr + GA + Tun30; Tun70: deep tunnel with 70% runoff absorbed. (For interpretation of the references to colour in this figure legend, the reader is referred to the Web version of this article.)

3.3. Cost-effectiveness comparison

Table 1 presents the comparative cost structure of the five basic solutions. The cost is accounted as the present value in 2013 RMB. The annual average cost (AAC) in the table indicates that the low impact solution of "green area expansion" has the lowest financial demand per year and the highest impact grey solution of Tun70 has the highest financial demand per year, respectively. Table 2 compares the cost-effectiveness of the above five basic solutions and the two combinations of "drainage enhancement + green area expansion" (D + G) and "drainage enhancement + green area expansion + deep tunnel with 30% runoff absorbed" (D + G + Tun30). Because the effectiveness measure in the comparison focuses on the risk reduction rate, the comparison clearly puts higher values on the deep tunnel solutions, of which Tun50 has the highest effectiveness-cost ratio. If the criterion of solution choice is that the risk reduction rate should be at least 85% on average, Tun70 will have the highest effectiveness-cost ratio.

4. Discussion

This study has proposed a planning-supporting tool which is capable of considering the entire cascade of factors from the uncertainties of future urban rainfall pattern and intensity, to the physical and economic damages caused by extreme rainfall events, and to the cost-effectiveness comparison of plausible solutions. The application of this synthesized trade-off analysis tool to the case of the reoccurrence in the 2050s of the extreme rainfall event on 13 September 2013 in Shanghai reveals a number of findings which are informative to urban planners and other stakeholders. First, the results show that drainage capacity decrease caused by sea-level rise and land subsidence will contribute the most to the worsening of future inundation risk in Shanghai. In contrast, future precipitation and urban rain island effect will have a relatively moderate contribution to the increase of the inundation depth and area. This result is also indirectly supported by a real rainstorm event happened in June 2015, which caused severe inundation in central Shanghai for days because high water level of rivers in the region prevented rainwater pumping from sewer systems into the river system. This finding should have general implications for other coastal cities sitting on river mouth. It means that it is important for urban planners in those cities to consider a scenario of a compound event in which an extreme storm surge under a sea level rise background takes place in an astronomical high tide period. Such an event would cause very severe flooding inside the city and bring disastrous impacts. To avoid regret in the near future, the mitigation and adaptation solutions should pay great attention to drainage standard increasing and drainage capacity strengthening, which should be ahead of the pace of sea level raise plus land subsidence.

The cost-effectiveness comparison in Section 3.3 brings up an important decision-making issue on the trade-offs between the grey infrastructure and the green solutions. The latter is usually known by varying names in different cultures, e.g. Low Impact Development (LID) in the US, Sustainable Urban Solutions (SUDS) in the UK, and Sponge City in China. The grey infrastructure usually possesses better protection standards in reducing inundation risks associated with the low return period events, but has a high level of negative impact on ecology and such negative impact is very difficult to be quantified. In sharp contrast, green solutions are typically effective in managing relatively high return period events, but beneficial to the local environment and ecology and such benefits are very difficult to be measured by monetary value (Palmer et al., 2015). Because it is difficult to measure the negative impact of grey infrastructure and the positive benefits of green solutions to the environment, planners typically under estimate both of them by a large margin. In recognition of this limitation, the solution of "drainage enhancement + green area expansion + deep tunnel with 30% runoff absorbed" (D + G + Tun30) becomes preferable to the solution of "deep tunnel with 70% runoff absorbed" (Tun70), given the integrative effect of D + G + Tun30 in reducing urban inundation risk by 85% (±8%) and in improving the local air quality and micro-climate.

Synthesized trade-off analysis of flood control solutions under future deep uncertainty asks for consolidation of various sets of data from different sources and for decision-making by the researchers in terms of solving conflicts across data sets and data sources, finding proxies for missing data, and identifying priorities and approximation margins in data-model fusion process. Our decisions on these important issues were made jointly with local experts and policy makers in a knowledge co-production process (Clark et al., 2016; Lempert et al., 2013; Liu et al., 2019; USGCRP, 2014). Field surveys and focus-group discussions were applied in the early stage of this work, which provided very useful information for knowing about the current protection standards, for illuminating the potential vulnerabilities, and for selecting the right adaptation solutions. Opinions of experts from different infrastructure sectors and scientific fields and discussions with stakeholders and policy makers also gave us inspiration for this Shanghai inundation application (Sun et al., 2019). For instance, expert opinions provided valuable insight for estimating the relationship between the drainage capacity and river water level and for using this relationship to approximate the drainage capacity decrease caused by sea-level rise and land subsidence. Discussions with policy makers and other stakeholders enabled us to know better their interests and priorities, which motivated our choices of solutions and key sources of uncertainties. This knowledge co-creation process also led to high trust in project results by policy makers. The results of the work were delivered to local decision-making authorities. Both the findings and the tool for the synthesized trade-off analysis of flood control solutions under future deep uncertainty were well appreciated by the authorities.

With increased demand for wise and visionary decisions in dealing with the risk and uncertainties posed by future climate change, there is an urgency to bridge the gap between the scientific research and practical applications. Although there is a myriad of

Table 1
Cost analysis of the five individual solutions.

Solutions	Initial Cost (million RMB)	Unit (km/km^2)	Maintenance and operations	Life span (year)	Life cycle cost (million RMB)	Salvage Value (Million RMB)	Annual Average Cost (million RMB/y)
Drainage	100/km	117.6	2%	50	13,427	52	269
Green	600/km^2	30.0	2%	70	17,988	36	257
Tun30	300/km	22.2	5%	50	14,070	29	281
Tun50	300/km	37.0	5%	50	23,451	49	469
Tun70	300/km	51.8	5%	50	32,831	68	657

Note: Drainage: drainage capacity enhancement; Green: green area increase; Tun30, Tun50, Tun70: deep tunnel with 30%, 50%, 70% runoff absorbed, respectively.

Table 2
Cost-effectiveness of the solutions.

	ARR (Average risk reduction rate, %)	PVC (million RMB/year)	ARR/PVC (percentage point/million RMB/year)
Drainage	25	269	0.093
Green area	26	257	0.101
Tun30	39	281	0.139
D + G	62	526	0.118
Tun50	74	469	0.158
D + G + Tun30	85	807	0.105
Tun70	87	657	0.132

Note: ARR: Average risk reduction rate. PVC: The present value of cost per year.

research running flood risk simulations and assessments in Shanghai and other mega-cities in the coastal areas, seldom can the detailed quantified solutions be digested by planners. This work, by integrating the simple but speedy SCS-CN based hydrological model into the framework of robust decision making under deep uncertainty, provides a practical and instructive example for bridging this important gap.

5. Conclusion

Precipitation change in the future is subject to deep uncertainties, especially in coastal mega-cities like Shanghai. Long-term planning to manage flood risk caused by extreme rainfall events is challenged by uncertainty in precipitation change and also in socioeconomic changes and contested stakeholder priorities. In this paper, we have proposed an integrated framework for a synthesized trade-off analysis of multiple flood-control solutions under the condition of deep uncertainties. We have demonstrated its operational ability with an application case study of central Shanghai, which focused on the reoccurrence in the 2050s of the extreme rainfall event on 13 September 2013. In the case study, we considered three uncertain factors, which include precipitation, urban rain island effect, and the decrease of urban drainage capacity caused by land subsidence and sea level rise. We built future extreme inundation scenarios based on the plausible ranges of changes in the above three uncertain factors and randomly selected 100 scenarios by using the Latin Hyper Cube (LHC) sampling method. We then estimated the inundation depth and area of these 100 rainfall scenarios under the condition of both existing infrastructure (reference runs) and enhanced infrastructure by introducing alternative sets of inundation-control solutions ("treated" runs). The inundation-control solutions include the increase of public green area, raising the standards of urban drainage system, construction of deep tunnel with varying levels of capacity, and the various combinations of the above basic solutions. The direct physical losses were calculated for the 100 reference runs and also for all "treated" runs, based on the depth-damage curves. The resultant large set of simulation results enabled us to calculate and then compare the risk-reduction performances of all possible solutions in different rainfall scenarios.

Two key results of these simulations and analyses are worth highlighting. First, drainage capacity decrease caused by sea-level rise and land subsidence will play a dominant role in worsening future inundation in central Shanghai. This finding in combination with others urges future infrastructure planning in coastal cities to pay a great attention to the compound event of an extreme storm surge under a sea level rise background occurring in a period of astronomical high tide. A "no regret" planning should be pro-active by strengthening the drainage capacity well ahead of the pace of sea level raise plus land subsidence. Second, although a performance comparison with a "flooding risk reduction rate" focus puts the solution of "deep tunnel with 70% runoff absorbed" (Tun70) ahead of "drainage enhancement + green area expansion + deep tunnel with 30% runoff absorbed" (D + G + Tun30), a consideration that the negative impact associated with deep tunnel construction on the environment and the environmental benefits of green areas are typically underestimated puts D + G + Tun30 as the top choice, which can reduce the future flood risk by 85% (±8%). This example enriches the literature on the performance evaluations between grey (e.g. traditional engineering structure) and green solutions in mitigating urban flood risk with reference to financial and ecological benefits and costs.

The experience of this research suggests that a synthesized trade-off analysis of alternative flood control solutions under future deep uncertainty cannot be accomplished by scientists alone, and it must be a knowledge co-creation process with decision makers and field experts. Such a knowledge co-creation process can ensure useable science for decision-making and lead to higher trust in project results by policy makers. Of course, the advantage of our decision supporting tool in running comprehensive evaluations for thousand combinations of scenarios-measures within one or a few days and with moderate demand for input data implies its disadvantage in lack of details at the grid-cell level. The second limitation is that the risk assessment in our work considered only the direct losses caused by inundation and ignored the indirect losses like interruptions to transportation and other urban functions, and then the sequential chain effect across urban social and economic sectors.

Declaration of competing interest

The authors declare that they have no known competing financial interests or personal relationships that could have appeared to influence the work reported in this paper.

Acknowledgement

This work was sponsored by the National Natural Science Foundation of China (Grant Nos. 41671113 and 51761135024), the Engineering and Physical Sciences Research Council of UK (Grant No. R034214/1), the Netherlands Organization for Scientific Research (NWO) (Grant No. ALWSD.2016.007), and the UK-China Research & Innovation Partnership Fund through the Met Office Climate Science for Service Partnership (CSSP) China as part of the Newton Fund (Grant No. AJYG-643BJQ). We gratefully acknowledge the valuable advices from Prof. Robert Lempert and Prof. Steven Popper of RAND Corporation. We thank Hanqing Xu for excellent research assistance and Hanwei Yang for assistance in Urban Inundation Model coding. Hengzhi Hu thanks the START program to sponsor his attendance at the RDM training workshop and visit to Rand Corporation.

Appendix A. Supplementary data

Supplementary data to this article can be found online at https://doi.org/10.1016/j.watres.2019.115067.

References

Aerts, J.C.J.H., Lin, N., Botzen, W.J.W., Emanuel, K., de Moel, H., 2013. Low-probability flood risk modeling for New York city. Risk Anal. 1–17.

Aerts, J.C.J.H., Botzen, W.J.W., Emnuel, K., et al., 2014. Evaluating flood resilience strategies for coastal megacities. Science 344 (6183), 473–475.

Ben-Haim, Y., 2004. Uncertainty, probability and information-gaps. Reliab. Eng. Syst. Saf. 85, 249–266.

Chen, Y., Samuelson, H.W., Tong, Z., 2016. Integrated design workflow and a new tool for urban rainwater management. J. Environ. Manag. 180, 45–51.

Chen, H.-P., Sun, J.-Q., Li, H.-X., 2017. Future changes in precipitation extremes over China using the NEX-GDDP high-resolution daily downscaled dataset. Atmosph. Ocean. Sci. Lett. 10 (6), 403–410. https://doi.org/10.1080/16742834.2017.1367625.

Chui, T.F.M., Liu, X., Zhan, W., 2016. Assessing cost-effectiveness of specific LID practice designs in response to large storm events. J. Hydrol. (Wellingt. North) 533, 353–364.

Chung, W.H., Wang, I.T., Wang, R.Y., 2010. Theory-based SCS-CN method and its applications. J. Hydrol. Eng. 15 (12), 1045–1058.

Clark, W.C., van Kerkhoff, L., Lebel, L., Gallopin, G.C., 2016. Crafting useable knowledge for sustainable development. Proc. Natl. Acad. Sci. U.S.A. 113 (17), 4570–4578.

CRED (Centre for Research on the Epidemiology of Disasters), 2014. EM-DAT—The International Disaster Database.

Fischer, G., Nachtergaele, F., Prieler, S., et al., 2008. Global Agro-Ecological Zones Assessment for Agriculture (GAEZ 2008). IIASA, Laxenburg, Austria and FAO, Rome, Italy.

Gu, W., Tan, J.-G., Chang, Y.-Y., 2015. Characteristics of heavy rainfall event in Shanghai region from 1981-2013. J. Met. Env. 31 (6), 107–114.

Haasnoot, M., Middelkoop, H., Offermans, A., Beek, E.V., Deursen, W.P.A.V., 2012. Exploring pathways for sustainable water management in river deltas in a changing environment. Clim. Change 115, 795–819.

Hadka, D., Herman, J., Reed, P., Keller, K., 2015. An open source framework for many objective robust decision making. Environ. Model. Softw 74, 114–129.

Hadley Centre, 2018. PRECIS: a Regional Climate Modelling System. https://www.metoffice.gov.uk/research/applied/international/precis.

Hallegatte, S., Green, C., Nicholls, R.J., Corfee-Morlot, J., 2013. Future flood losses in major coastal cities. Nat. Clim. Chang. 3, 802–806.

Han, J.C., 2014. Optimization of upgrading schemes of drainage systems by InfoWorks ICM software. China Water & Wastewater 30 (11), 34–38.

Han, J.Y., Baik, J.J., Lee, H., 2014. Urban impacts on precipitation. Asia-Pac. J. Atmos. Sci. 50, 17–30.

He, F.F., 2012. Characteristics of torrential rain in Shanghai from 1980s. In: Proceedings of the Urban Meteorology Forum—Urban and Climate Change, Shenzhen, China, 24–25 November 2012, pp. 10–17 (In Chinese).

He, F.F., Zhao, B.K., 2009. The characteristics of climate change of torrential rains in Shanghai region in recent 30 years. Adv. Earth Sci. 24, 1260–1267 (In Chinese).

Hooshyar, M., Wang, D., 2016. An analytical solution of Richards' equation providing the physical basis of SCS curve number method and its proportionality relationship. Water Resour. Res. 52, 6611–6620. https://doi.org/10.1002/2016WR018885.

Huong, H.T.L., Pathirana, A., 2013. Urbanization and climate change impacts on future urban flood risk in Can Tho city. Vietnam. Hydrol. Earth Syst. Sci. 17, 379–394.

Innovyze, 2018. InfoWorks ICM Is an Advanced Integrated Catchment Modeling Software. https://www.innovyze.com/en-us/products/infoworks-icm.

IPCC, 2014. Climate Change 2014: Impacts, Adaptation, and Vulnerability. Cambridge University Press, Cambridge.

ISO Guide 31000, 2009. Risk Management - Principles and Guidelines. http://ehss.moe.gov.ir/getattachment/56171e8f-2942-4cc6-8957-359f14963d7b/ISO-31000.

Jenkins, K., Surminski, S., Hall, J., et al., 2017. Assessing surface water flood risk and management strategies under future climate change: insights from an agent-based model. Sci. Total Environ. 595, 159–168.

Jiang, Z.H., Li, W., Xu, J., et al., 2015. Extreme precipitation indices over China in CMIP5 models. Part I: model evaluation. J. Clim. 28 (21), 8603–8619.

Kasprzyk, J.R., Nataraj, S., Reed, P.M., Lempert, R.J., 2013. Many objective robust decision making for complex environmental systems undergoing change. Environ. Model. Softw. 42, 55–71.

Ke, Q., 2014. Flood Risk Analysis for Metropolitan Areas – A Case Study for Shanghai. PhD Dissertation. Technology of Delft University, Department of Hydraulic Engineering.

Kharin, V.V., Zwiers, F.W., Zhang, X., Hegerl, G.C., 2007. Changes in temperature and precipitation extremes in the IPCC ensemble of global coupled model simulations. J. Clim. 20 (8), 1419–1444.

Kusaka, H., Nawata, K., Suzuki-Parker, A., Takane, Y., Furuhashi, N., 2014. Mechanism of precipitation increase with urbanization in Tokyo as revealed by ensemble climate simulations. J. Appl. Meteorol. Climatol. 53, 824–839.

Lee, J.W., Hong, S.Y., Chang, E.C., et al., 2014. Assessment of future climate change over East Asia due to the RCP scenarios downscaled by GRIMs-RMP. Clim. Dyn. 42 (3–4), 733–747.

Lempert, R.J., McKay, S., 2011. Some thoughts on the role of robust control theory in climate-related decision support. Clim. Change 2011 (107), 241–246.

Lempert, R.J., Kalra, N., Peyraud, S., 2013. Ensuring Robust Flood Risk Management in Ho Chi Minh City. RAND, Santa Monica, CA.

Li, W., Jiang, Z., Xu, J., et al., 2016. Extreme precipitation indices over China in CMIP5 models. Part II: probabilistic projection. J. Clim. 29 (24), 8989–9004.

Liang, P., Ding, Y.H., 2017. The long-term variation of extreme heavy precipitation and its link to urbanization effects in Shanghai during 1916–2014. Adv. Atmos. Sci. 34, 321–334.

Liao, Z.L., He, Y., Huang, F., Wang, S., Li, H.Z., 2013. Analysis on LID for highly urbanized areas' waterlogging control: demonstrated on the example of Caohejing in Shanghai. Water Sci. Technol. 68 (12), 2559–2567.

Liu, D.-G., 2004. Possible impacts of relative sea level rise in the coastal areas in China. Mar. Forecasts 21 (2), 21–28 (in Chinese).

Liu, J., Bawa, K.S., Seager, T.P., Mao, G., Ding, D., Lee, J.S.H., Swim, J.K., 2019. On knowledge generation and use for sustainability. Nat. Sustain. 2, 80–82.

Löwe, R., Urich, C., Domingo, N., et al., 2017. Assessment of urban pluvial flood risk and efficiency of adaptation options through simulations – a new generation of urban planning tools. J. Hydrol. 355–367.

Mauser, W., Klepper, G., Rice, M., Schmalzbauer, B.S., Hackmann, H., Leemans, R., Moore, H., 2013. Transdisciplinary global change research: the co-creation of knowledge for sustainability. Curr. Opin. Environ. Sustain. 5 (3–4), 420–431.

Meadow, A.M., Ferguson, D.B., Guido, Z., Horangic, A., Owen, G., Wall, T., 2015. Moving toward the deliberate coproduction of climate science knowledge. Weather Clim. Soc. 7 (2), 179–191.

Mishra, S.K., Singh, V.P., 2003. Soil Conservation Service Curve Number (SCS-CN) Methodology. Kluwer Academic Publishers, Dordrecht.

Muis, S., Güneralp, B., Jongman, B., Aerts, J.C.J.H., Ward, P.J., 2015. Flood risk and adaptation strategies under climate change and urban expansion: a probabilistic analysis using global data. Sci. Total Environ. 538, 445–457.

Palmer, M.A., Liu, J., Mattews, J.H., Mumba, M., D'Odorlco, P., 2015. Manage water in a green way. Science 349 (6248), 584–585.

Paul, S., Ghosh, S., Mathew, M., Devanand, A., Karmakar, S., Niyogi, D., 2018. Increased spatial variability and intensification of extreme monsoon rainfall due to urbanization. Sci. Rep. 8, 3918.

Poelmans, L., von Rompaey, A., Ntegeka, V., Willems, P., 2011. The relative impact of climate change and urban expansion on peak flows: a case study in central Belgium. Hydrol. Process. 25, 2846–2858.

Rosenzweig, C., Solecki, W.D., Hammer, S.A., Mehrotra, S., 2011. Climate Change and Cities: First Assessment Report of the Urban Climate Change Research Network. Cambridge University Press, Cambridge, UK.

Sekovski, I., Armarolim, C., Calabrese, L., Mancini, F., Stecchi, F., Perini, L., 2015. Coupling scenarios of urban growth and flood hazards along the Emilia-Romagna coast (Italy). Nat. Hazards Earth Syst. Sci. 15, 2331–2346.

Shanghai Municipal Government, 2017. The 13th five-year plan of Shanghai on water resource protection and utilization and flooding control (in Chinese). http://fgw.sh.gov.cn/wcm.files/upload/CMSshfgw/201706/201706050327041.pdf.

Shanghai Urban Planning and Land Resource Administration Bureau, 2018. Shanghai Master Plan 2017-2035. The version for public reading is available at: http://www.shanghai.gov.cn/newshanghai/xxgkfj/2035004.pdf.

Shimoju, R., Nakayoshi, M., Kanda, M., 2010. Case analyses of localized heavy rain in Kanto considering urban parameters (in Japanese with English abstract). Ann. J. Hydraul. Eng. 54, 349–354.

Souma, K., Tanaka, K., Suetsugi, T., et al., 2013. A comparison between the effects of artificial land cover and anthropogenic heat on a localized heavy rain event in 2008 in Zoshigaya, Tokyo, Japan. J. Geophys. Res. Atmos. 118 (11) https://doi.org/10.1002/jgrd.50850, 600–11,610.

Statistic Year Book of Shanghai, 2013, 2014, 2015. Shanghai Statistics Bureau. (In Chinese)..

Sun, Landong, Tian, Z., Zou, H., Shao, L., Sun, Laixiang, Dong, G., Fan, D., Huang, X., Frost, L., Fox-James, L., 2019. An index-based assessment of perceived climate risk and vulnerability for the urban cluster in the Yangtze River Delta Region of China. Sustainability 11, 2099. https://doi.org/10.3390/su11072099.

Teng, J., Jakeman, A.J., Vaze, J., et al., 2017. Flood inundation modelling: a review of methods, recent advances and uncertainty analysis. Environ. Model. Softw 90, 201–216.

Thomson, A.M., Calvin, K.V., Smith, S.J., et al., 2011. RCP4.5: a pathway for stabilization of radiative forcing by 2100. Clim. Change 109, 77–94. https://doi.org/10.1007/s10584-011-0151-4.

United Nations, Department of Economic and Social Affairs, Population Division, 2018. The World's Cities in 2018 – Data Booklet (ST/ESA/SER.A/417).

USGCRP (U.S. Global Change Research Program), 2014. National climate assessment, chapter 26: decision support. https://nca2014.globalchange.gov/downloads.

Voorberg, W.H., Bekkers, V.J., Tummers, L.G., 2015. A systematic review of co-creation and co-production: embarking on the social innovation journey. Public Manag. Rev. 17 (9), 1333–1357.

Wang, X., Yin, Z.-E., Chi, X.-X., Yin, J., 2015. Characteristics of different magnitude precipitation change in Shanghai during 1961—2010. J. Earth Env. 6 (3), 161–167 (In Chinese).

Wang, J., Yi, S., Li, M., Wang, L., Song, C., 2018. Effects of sea level rise, land subsidence, bathymetric change and typhoon tracks on storm flooding in the coastal areas of Shanghai. Sci. Total Environ. 621, 228–234.

Westra, S., Alexander, L.V., Zwiers, F.W., 2013. Global increasing trends in annual maximum daily precipitation. J. Clim. 26, 3904–3918.

Westra, S., Fowler, H.J., Evans, J.P., Alexander, L.V., Berg, P., Johnson, F., Kendon, E.J., Lenderink, G., Roberts, N.M., 2014. Future changes to the intensity and frequency of short duration extreme rainfall. Rev. Geophys. 52, 522–555. https://

doi.org/10.1002/2014RG000464.
Wu, P., Christidis, N., Stott, P., 2013. Anthropogenic impact on Earth's hydrological cycle. Nat. Clim. Chang. 3, 807–810.
Wu, J., Yang, R., Song, J., 2018. Effectiveness of low-impact development for urban inundation risk mitigation. Nat. Hazards Earth Syst. Sci. 18, 2525–2536. https://doi.org/10.5194/nhess-18-2525-2018.
Yuan, Y., Xu, Y.-S., Arulrajah, A., 2017. Sustainable measures for mitigation of flooding hazards: a case study in Shanghai, China. Water 9, 1–16. https://doi.org/10.3390/w9050310, 310.